

Runaway Electrons in JET – Summary on RE Data after the End of JET **Operations**

V.V. PLYUSNIN(1), C. REUX, V.G. KIPTILY, A.E. SHEVELEV, P. J. LOMAS, E. JOFFRIN, A. HUBER, O. FICKER, S. GERASIMOV, S. JACHMICH, A. BOBOC, J. MLYNAR, M. LEHNEN, THE EUROFUSION TOKAMAK EXPLOITATION TEAM+ AND JET CONTRIBUTORS*

EUROFusion Consortium, JET, Culham Science Centre, Abingdon, OX14 3DB, UK

(1) Instituto de Plasmas e Fusão Nuclear, Instituto Superior Tecnico, Universidade de Lisboa, Lisboa, Portugal; *See the author list of "Overview of T and D-T results in JET with ITER-like wall" by C.F. Maggi et al 2024 Nuclear Fusion 64 112012

+See the author list of "Overview of the EUROfusion Tokamak Exploitation programme in support of ITER and DEMO" by E. Joffrin et al 2024 Nuclear Fusion 64 112019

INTRODUCTION.

Disruptive terminations of plasma discharges pose severe threats to the device integrity in future operations of International Thermonuclear Experimental Reactor (ITER). Disruptions can cause dangerous excessive electromagnetic forces, heat loads and generation of the intense beams of relativistic runaway electrons (RE). Localized interaction of such beams with surrounding plasma facing components (PFC) inevitably will result in their inacceptable damage. To avoid/suppress RE generation and mitigate other disruption detrimental consequences the Disruption Mitigation System (DMS) is under design in ITER. It is based on impurities injection in the form of solid shattered pellets (\mathbf{SPI}). Development of DMS requires advanced understanding of the physics of RE and their interaction with plasma, solid pellets and neutral gases (fuel and impurities). For this purpose, the parameters of disruption generated RE collected during disruptions till to the end of JET operations in 2023 were compiled into joint database. It includes parameters of more than 2000 RE generation events in major disruptions before (JET with ${f O}$ riginal ${f P}$ lasma ${f S}$ hape, JET OPS, Splasma≤ 7.8 m²) and after divertor installation, with metal and carbon limiters and with ITER-like Wall (JET-C and JET-ILW, Spl ≤ 4.7 m²), see table 1, in spontaneous disruptions and those triggered by slow gas puff, MGI and SPI. This report presents a survey and present status of RE data analysis in JET.

HISTORICAL SUMMARY ON RE GENERATION DURING JET OPERATIONS

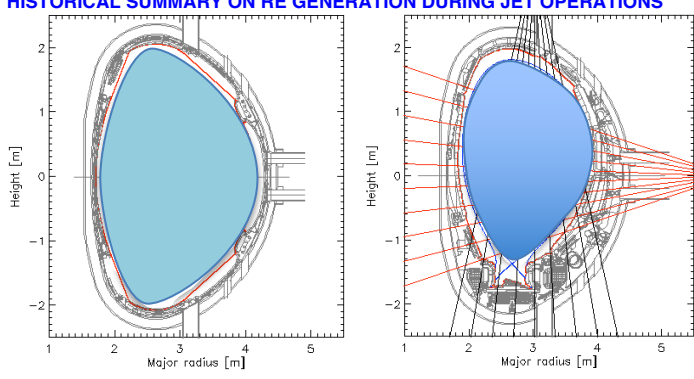


FIG. 1 The JET plasma cross-sections with original shape before divertor installation (JET OPS, $S_{pl} \le 7.8 \text{ m}^2$, left chart) and with divertor coils installed inside

| of the vacuum vesser (of a divertor, Spi & 4.7 m , highly. | | | |
|--|-------------------------------------|-----------|---------------------|
| Operational phases & plasma | Period | Last shot | Detected RE |
| configurations, PFC materials and diverto | r | number | generation |
| configurations | | | events |
| JET- Original Plasma Shape (JET-OPS) | Operations till to August 1987 | #12106 | ≈ 320 events |
| JET-OPS, Limiter, X-Point (SN, DN) | August 1987 - February 1992 | #28791 | ≈ 560 events |
| JET-C – Divertor MKI + CFC tiles | March 1994 - June 1995 | #35778 | ≈ 130 events |
| JET-C – Divertor MKIIA, AP + CFC tiles | May 1996 – Feb 1998 – Sept 1998 | #45155 | ≈ 220 events |
| JET-C – Divertor MKIIGB +CFC tiles | July 1998 - March 2001 | #54549 | ≈ 250 events |
| JET-C – Divertor MKIIGB SR + CFC tiles | Jul 01 - Mar 04; Aug 05 - Apr 07 | #63445 | ≈ 150 events |
| JET-C – Divertor MKII HD + CFC tiles | Carbon wall ends 23-Oct- 2009 | #79853 | ≈ 150 events |
| JET with ITER Like Wall (ILW) + Divertor | ILW Experiments – from July 2011 | #105929 | ≥ 340 events |

TABLE 1. A survey of JET operation stages and number of RE generation events detected during

- ≈ 340 disruptions with REs at disrupted currents up to 3MA during JET-ILW SPI-MGI experiments have been dedicated to studies of interaction of RE beams with MGI or SPI of D₂ and He. Ar. Ne. Xe. Kr or their mixture with D₂.
- · All other unintentional disruptions in JET-ILW have been mitigated with MGI

INSTRUMENTATION

RE interacting with plasma particles and PFC lose energy and produce the Xray emission in a wide energy range: from soft X-rays (SXR) till to multi-MeV energies of hard X-rays (HXR) or γ -rays; HXR energy corresponds to the energy of electrons: $E_{HXR} \le E_{RE_MAX} - m_e c^2$; Photo-neutrons (nY) are also produced when γ 's interact with PFC and plasma particles and when the photon energy is higher than the neutron bound energy of target nuclei ε_n : $E_n = E_{HXR} - \varepsilon_n$. Binding energies for different materials in JET are: $D_2 - 2.2$ MeV; Be -1.7 MeV; C - 18.7 MeV; Ar - 9.9MeV; Ni – 12.0 MeV; Cu – 10.6 MeV; W – 7.4 MeV, Ne – 8 MeV

Figure 2 presents layout of diagnostics sets used for measurements of RE parameters in the JET experiments: 5 scintillation time-resolved HXR monitors, for neutron rates fission chamber monitors (235U and 238U) at 3 different locations (N1, N2 & N3 - Oct. 2,6,8) operating in a current mode with 0.0001 sec time resolution (Figure 2, left chart).

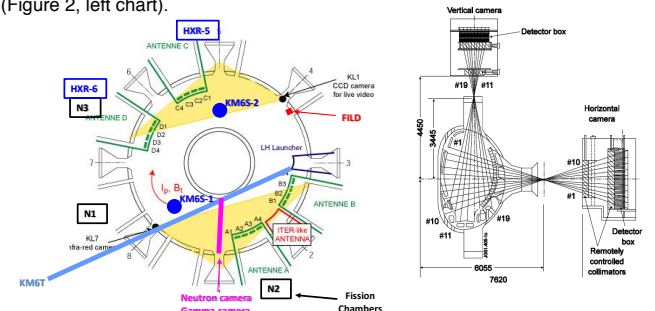
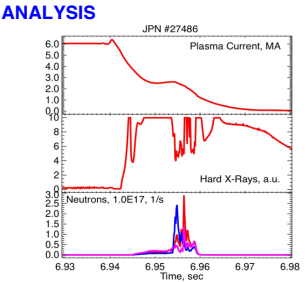
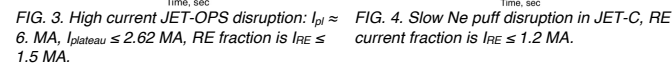


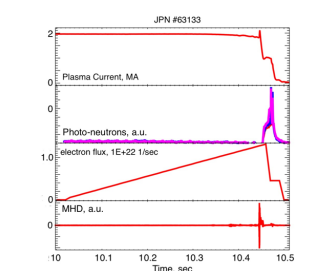
FIG. 2 Layout of JET diagnostics used in RE studies (left chart) and JET neutron/g-profile monitor setup (right chart): 2 cameras, vertical and horizontal, with 9 and 10 detectors (corresponding Lines of Sights (LoS) are shown).

Horizontally and vertically viewing NaI(TI), Bi₄GeO₁₂ (aka BGO, Oct. 8) and LaBr₃ spectrometers; JET neutron/γ-rays profile monitor in Oct.1 (Figure 2, right chart). Each camera has 2 detectors: NE213 - for neutron and HXR measurements, and CsI detector for HXR registration. Fan-shaped array of remotely adjustable collimators with two apertures (Ø10 & 21 mm) provide the space resolution: ~8 (or ~15) cm (in the centre). CsI(TI) scintillators (for HXR/gammas) equipped with fast digital data acquisition system: t ≈ 1 ms. HXR 2D imaging system enables the reconstruction of evolution in time and space of the RE beam; Several sets of SXR cameras have been used to produce SXR tomography of the RE beams images in-flight.

MAIN SCENARIOS OF DISRUPTIONS IN JET AND REFERENCE MODEL FOR







current fraction is I_{RE} ≤ 1.2 MA

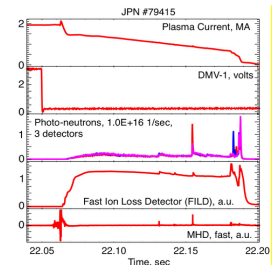


FIG. 5. MGI Disruption in JET-C Ipla

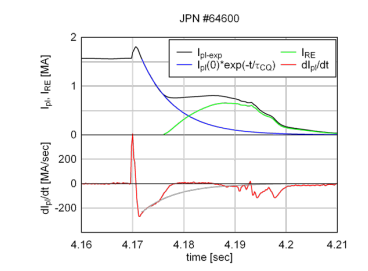
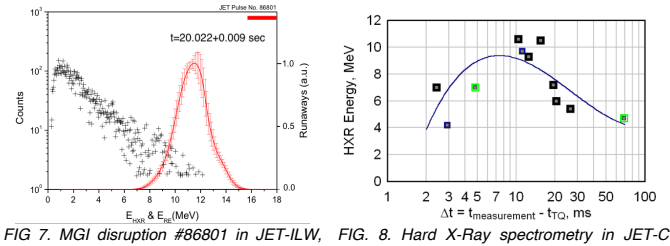
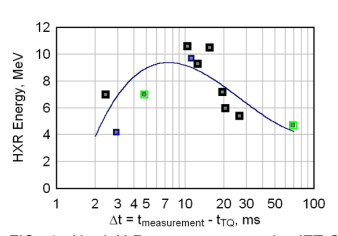


FIG. 6. Reference model for analysis of RE

MEASUREMENTS OF RE ENERGY AND REDF IN JET DISRUPTIONS

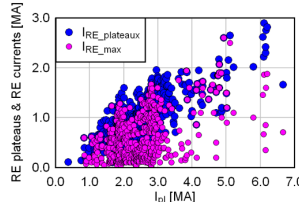


HXR spectrum: NaI(TI) detector (raw data, black crosses); reconstructed RE energy spectrum using de-convolution procedure



disruption. NaI(TI) detector, fast DAQ. integrated signal from vertical Line-of-Sight. Maximal RE energy E_{MAX} vs. time from the

MAIN TRENDS IN RUNAWAY ELECTRON PARAMETERS MEASRED IN ALL SCENARIOS OF MAJOR DISRUPTIOS IN JET



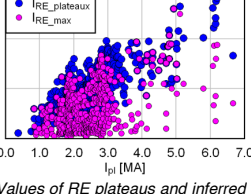
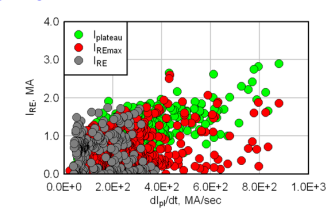


FIG 9. Values of RE plateaus and inferred RE FIG.9. Dependence of RE current plateaus current fractions plotted vs. disrupted plasma



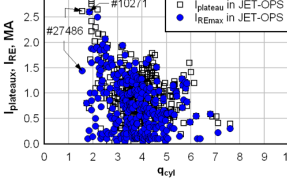
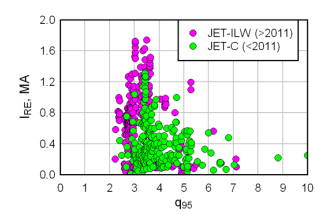
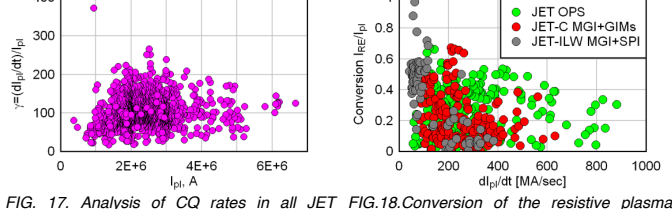
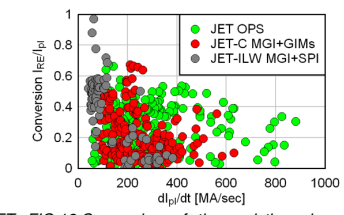


FIG.11. JET-OPS data on generated RE FIG.12. Data on RE currents generated in plateaus and calculated runaway current JET-C and JET-ILW disruption scenarios fractions plotted vs. q(a)



plotted vs. qos (EFIT data)





current into RE one vs. on plasma current time derivative in all disruption scenarios

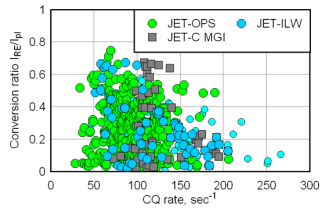


FIG. 15. Conversion ratio vs. CQ rates for all stages of JET operations

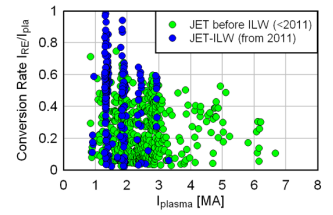


FIG.16. Conversion ratio dependence on disrupted plasma currents plotted for all JET

E-mail: vladislav.plyusnin@ipfn.ist.utl.pt

- ⇒ The measured energies (E_{MAX} ≤ 10÷12 MeV) are too low in comparison to values expected from: $\gamma = \sqrt{1 + \left(\left(\frac{e}{m_e c} \cdot \int E_{\parallel 0}(t) dt\right)^2\right)} \sim 50 \div 60$ (for electric field ~ 50 V/m, which is acting during 0.002-0.004 sec).
- Observed controversy requires an additional analysis described dynamics including numerical data processing and modelling.
- Description Evaluation of RE density from measured or deduced runaway current fractions. In particular, assessment of RE density values provided necessary data on evaluation of RE distribution function. Fig 15 presents data on RE density evaluated from given values of RE currents for different values of critical energy of runaway process (represented by Lorentz parameter γ_0): $I_{RE}=\frac{ec}{\gamma_0}\sqrt{\gamma_0^2-1}\frac{n_{RE}}{2\pi R_0}$

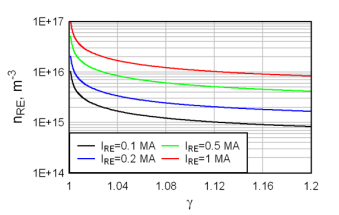


FIG. 15. RE density in runaway beams with different currents depending on estimated runaway critical energies. RE density has been assessed from $N_e=2\pi R_0 I_{RE_tot}/(ec\beta)$

EFFECT OF CURRENT QUENCH **EVOLUTION AND PLASMA GEOMETRY DYNAMICS ON RE GENERATION: JET**

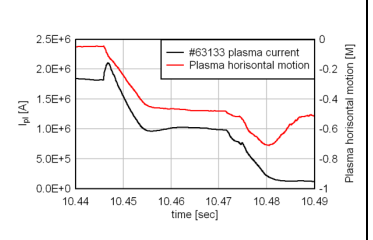
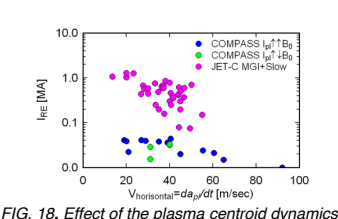
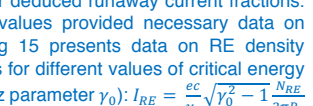
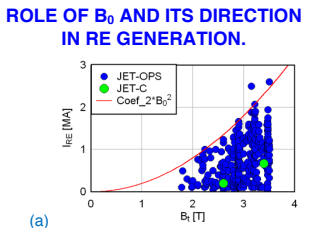


FIG. 17. Evolutions of plasma centroids (PPOX) and runaway current in JET disruption: JPN #63133



in horizontal direction (V_{horizontal}=da_{pl}/dt) on RE generation efficiency in tokamaks





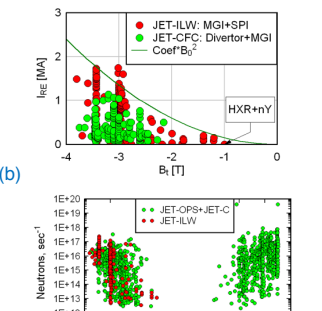


FIG. 16. RE currents plotted as maximal IR vs. B_t for different directions [(a) - positive; (b)-negative], (c) - photoneutrons data in

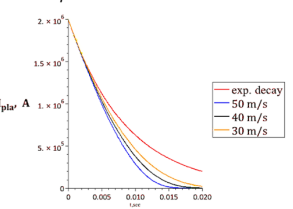


FIG. 19. Evolution of CQ calculated with Eas.(2-3) for different velocities of horizontal plasma toroid motion

Disrupted plasmas move fast in space (vertical and horizontal) with changes in many parameters: radius, total inductance, magnetic flux, etc. These evolutions revealed definite effect on RE generation dynamics.

Simulations on disruption evolutions were carried out using following model:

$$\frac{dn_{RE}}{dt} = \lambda_R + (\gamma_{AV} - \frac{1}{\tau_{RE}}) \cdot n_{RE}$$
 (1),
$$I_{pla}(t) + \frac{\iota_p(t)}{R_{pl}(t)} \frac{dI_p}{dt} + 0.5 \cdot I_p(t) \frac{dL_p}{dt} = 0$$
 (2),
$$\rho \frac{dv}{dt} = \sum_i F_i$$
 (3);

Where
$$F_1 = 2\pi R(t)I_p(t) \cdot B_V$$
, $B_V = \mu_0 \frac{I_p(0)}{4\pi R_0} \left(\ln \frac{8R_0}{a_{pl}(0)} + \beta_p(0) + \frac{I_l(0)}{2} + 2 \right)$, $F_2 = \mu_0 \frac{I_p^2(t)}{2} \left(\ln \frac{8R(t)}{a_p(t)} + \beta_p^*(t) + \frac{I_l^*(t)}{2} + 2 \right)$; $\beta_p^*(t) = \beta_p(t) + \beta_{RE}(t)$; $N_{RE} = 2\pi R_0 \frac{I_{RE}}{ec\beta}$; $L_p(t) = \mu_0 R_0(t) \left(\ln \left(\frac{8R_0(t)}{a_p(t)} \right) + \beta_p^*(t) + \frac{I_l}{2} - 2 \right)$, $I_l = \ln(1.65 + 0.89c)$

$$\gamma_{AV} = \frac{\frac{e}{mc}}{\ln \Lambda \sqrt{\frac{3}{\pi}} (Z_{eff} + 5)} \cdot \left(E_0(t) - E_{CR_{-\infty}} \cdot \frac{\gamma_0^2}{\gamma_0^2 - 1} \right) \qquad \beta_{RE}(t) = 8\pi^2 \alpha_p^2 n_{RE} \frac{m_e c^2 \cdot (\gamma_0^2 - 1)}{2\mu_0 I_p^2 \cdot \gamma_0^2}$$

$$\frac{dL_p}{dt} = \mu_0 \cdot \left[\frac{dR_0(t)}{at} \cdot \left(\ln \left(\frac{8R_0(t)}{a_{pl}(t)} \right) - 2 \right) + R_0(t) \left(\frac{dR_0(t)}{at} - \frac{da_{pl}(t)}{at} \right) \right], \frac{dR_0(t)}{R_0(t)} < 0, \frac{da_{pl}(t)}{a_{pl}(t)} < 0;$$

$$2\pi R_0 E_{\parallel 0}(t) = -(L_{tot}(t) \frac{dI_p}{dt} + 0.5I_p(t) \frac{dL_{tot}}{dt} \right), \qquad \gamma_0^2 = 1 + \left[\frac{e}{mc} \int E_0(t) dt \right]^2$$

Collected data on RE generation events (>2000 in total) in JET disruptions covers all stages of JET operations. Runaways have been generated during spontaneous or deliberate disruptions in different plasma configurations: circular or elongated. limiter or divertor, etc. Extended analysis of RE database established key dependencies of main post-disruption RE parameters, such as, RE densities, currents and current conversion ratios (IRE/IpI) on pre-disruption plasma currents, plasma current time derivatives, CQ rates, safety factor q95/q(a), pre-disruption density, temperature, etc. In several experiments with MGI and SPI the HXR/y and photo-neutrons diagnostics measured maximal energies of runaways EMAX ≤ 10÷12 MeV. Analysis of SPI experimental results and data from experiments with MGI using different DMVs revealed different influence on disruption dynamics and RE generation. One of the important results from the data-base analysis is observation of clear threshold in RE generation on CQ rates. A decreasing trend in conversion ratio I_{RE}/I_{pl} has been established vs. main parameters, such as predisruption plasma currents, plasma current time derivatives and CQ rates. Presented data-base on RE in JET requires further extended study including analysis of the disruption phenomenology and numerical simulations of runaway generation dynamics.

REFERENCES

[1] Harris G.R.1990 Preprint JET-R(90)07

[2] O.N. Jarvis et al. 1988 Nuclear Fusion 28 1981 [3] R.D. Gill et al. 2002 Nuclear Fusion 42 1039

[4] V. V. Plyusnin et al. 2006 Nuclear Fusion 46 277











